HADRONIC JOURNAL 48, 307 - 339 (2025)
DOI 10.29083/HJ.48.03.2025/SC307

DIRECT OBSERVATION OF UNUSUAL PROPERTIES OF STRONG INTERACTIONS INACCESSIBLE BY ACCELERATOR

V.G. Plekhanov
Fonoriton Sci. Lab.
Garon Ltd, Tallinn 11413, Estonia
vgplekhanov@proton.me

Received August 6, 2025
Revised August 13, 2025

Abstract

This brief review is devoted to the manifestation in the mass isotope effect of the nonlinear dependence of the strong interaction on the neutron - binding energy which may indicated the manifestation of the new unknown force. A striking new manifestation of the strong interaction is the acquisition of mass by massless fermions (leptons) of Dirac in graphene. We emphasize that the study of the isotope effect remains at the forefront of nuclear and high energy physics.

Keywords: strong interaction, hadrons, quarks, gluons, excitons, phonons, quantum electrodynamics, quantum chromodynamics

Copyright © 2025 by Hadronic Press, Inc., Palm Harbor, FL 34684, USA

I. **Introduction.**

Modern physics distinguishes three fundamental properties of atomic nuclei: mass , spin (and related magnetic moment), volume (surrounding field strength), which are the source of isotope effect. The stable elementary particles (electrons, protons and neutrons) have intrinsic properties. Some of these properties such as mass and electrical charge are the same for macroscopic objects. Some are purely quantum mechanical and have no macroscopic analog. Spin is an intrinsic angular momentum associated with elementary particles. The spin angular moment of an electron, measure along any particular direction, can only take on the values $\hbar/2$ or $-\hbar/2$. The nuclear magnetic moment associates with nuclear spin and produces the magnetic interaction with its environment. The ability to manipulate and control electron and/or nucleus spin in semiconductor devices provides a new route to expand the capabilities of inorganic semiconductor - based electronics and to design innovative devices with potential application in quantum computing.

Among the prime premises of quantum physics is the principle of indistinguishability of elementary particles. All electrons are by definition 'the same' and hence, after two (or more) electrons interact, it is possible to say 'who is who'. The same applies to other elementary particles and even identical atoms (e.g., two ^{70}Ge atoms are indistinguishable). Not so for isotopes. Due to their mass difference, various isotopes of the same chemical element (e.g., ^{70}Ge and ^{76}Ge) are classical distinguishable particles. Within the framework of statistical thermodynamics, this classical distinguishability of isotopes renders isotopic mixtures a prime illustrative tool for a discussion of the Gibbs paradox. The latter refers to the (alleged) discontinuity of entropy upon the mixture of two slightly different species.

The discovery of the neutron by Chadwick in 1932 may be viewed as the birth of the strong interaction: it indicated that nuclei consists of protons and neutrons and hence the presence of a force that holds them together, strong enough to counteract the electromagnetic repulsion. It is well - known that most of the mass of an atom is concentrated in the tiny nucleus surrounded by a cloud of electrons. The nucleus in turn is formed of protons and neutrons, but these are not elementary either (see, e.g. Fig. 1 in Chapter 2 of [1]). They are actually composed of even smaller particles, called quarks. Gradually over the last century physicists built up what we now call the Standard Model (SM) of particle physics [2], which describes the particles we now believe to be fundamental and their interaction. The SM includes Quantum

Chromodynamics (QCD), the theory of the strong nuclear interactions. According to this model, all matter is built from a small number of fundamental spin 1/2 particles, or fermions; six quarks and six leptons (see below Table 1). The leptons carry integral electric charge. The electron e with unit negative charge is familiar to everyone, and the charged leptons are the muon μ and tauon τ. These are heavy versions of the electron. The neutral leptons are called neutrinos, denoted by the generic symbol ν. A different 'flavor' of neutrino is paired with each 'flavor' of charged lepton, a indicated by the subscript. For example, in nuclear β - decay, an electron e is emitted together with an electron - type neutrino, ν_e. The charged muon and tauon are both unstable, and decay spontaneously to electrons, neutrinos and other particles (see, e.g. [3]). The mean lifetime of the muon is $2.2\text{x}10^{-6}$s, that of the tauon only $2.9\text{x}10^{-13}$s. In the theory of strong interquark forces, QCD, there are six types of strong charge, called color charges; color is just a name for an internal degree of freedom. A quark can carry one of three primary colors (say red, blue and green), and its antiquark then carries the corresponding anticolor. The quark combinations called hadrons have no color. A baryon (proton or neutron) of one red, one blue and one green quark, the combination being white (i.e. colorless) Similarly, a meson consisting of a quark of a particular color and antiquark of that anticolor, is also colorless. Gluons, unlike photons, carry a color charge, consisting of one color and one anticolor.

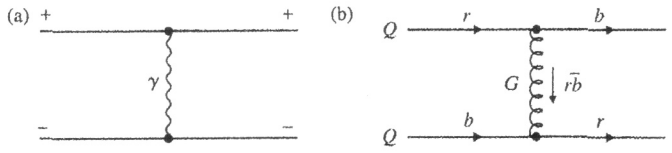

Fig. 1. Comparison of the Feynman diagrams of electromagnetic (a) and strong (b) interactions. The electromagnetic interaction in (a) involves two types of electric charge, (+) and (-) is mediated by an uncharged photon. In (b) the strong interquark force involves six types of color charge. The diagram depicts the interaction of a red quark with a blue quark via the exchange of a red - antiblue gluon.

As an example , Fig. 1[b]shows a red quark r interacting with a blue quark b via

exchange of $r\bar{b}$ gluon. Note that the gluon carrier itself is endowed with a color charge ($r\bar{b}$ in our case). On this account, gluons have self - interaction, with triple (and quadrupole) gluon vertices [4]. This marks a crucial difference from Quantum Electrodynamics (QED), where the photon uncharged and there is no first - order photon - photon interaction [4]. In the jargon, QED is said to be an Abelian, and QCD is a non - Abelian theory [5]. Since the gluons carry one color and one anticolor, there should be $3^2 = 9$ possible color combinations. However, one of these turns out to be a colorless singlet (in the form $r\bar{r} + b\bar{b} + g\bar{g}$ [3]), leaving eight active gluon states: so - called eight - fold way [6j].

The diagram of Fig. 1 is drawn for the case of single – gluon exchange, but taking into account that strong constant coupling $\alpha_s \sim 1$, multiple exchanges, involving terms α_s^2, α_s^3, ... must also be very probable. However, it turns out that for violent 'close' collisions at very high q^2, $\alpha_s \ll 1$ and single - gluon exchange is a good approximation, while at low q^2 or, equivalently, larger distances, the coupling becomes very large and the theory is incalculable. This large - distance behavior is presumably linked with of confinement of quarks and gluons inside hadrons. Since gluons are massless, one might expect the static QCD potential to have a similar: 1/r, form to that in QED. In fact the quark - antiquark potential is often taken to be of the form

$$V_s = -\frac{4}{3}\frac{\alpha_s}{r} + kr \qquad (1)$$

where the first term, dominating at small r, arises from single - gluon exchange. It is similar to the Coulomb potential between two unit charges of

$$V_{em} = = -\frac{\alpha}{r} \qquad (2)$$

The factor 4/3 in (1) is plausible in view of the fact that there eight color gluon states, to be averaged over three quark colors, giving factor 8/3 as compared with QED (one 'color' of photon and one fermion charge). This has to divided by 2 because, for historical reasons [4], a factor 2 enters into definition of α_s in terms of the square of the strong color charge. However, at larger distances the second term in (1) is dominant and is responsible for quark confinement. The value of k is about o.85 GeVfm^{-1}. In equation (1) the attractive force at large r is dV/dr = k = 085 Gevfm^{-1}

[4]. The estimation of the k equals k = 13.9 tonnes weight - a great deal for those tiny quarks, each weighting less than 10^{-24} gm because gluons carry a color charge (unlike photons which are uncharged) there is a strong gluon - gluon interaction. If one tries to pull apart the two quarks, the energy required to do so grows linearly with the string (distance) as in (1), and eventually it requires less energy to produce another quark - antiquark pair, thus involving two short string instead one long one. Thus even the most violent efforts to separate quarks just result in production of lot of quark - antiquark pairs (mesons) [3]. Since the protons and neutrons which make up the nucleus are themselves considered to be up of quarks are considered to be held together by the color force [3], the strong force between nucleons may be considered to be residual color force (see e.g.[1]).

In modern physics, particles are classified into two groups based on their properties. There are known as fermions and bosons. In the SM fermions are the fundamental particles of matter. Elementary fermions are leptons (see Table 1).

Table 1. Quarks and leptons

	Family			Electric charge (e)
	1	2	3	
Leptons	e^-	μ^-	τ^-	- 1
	ν_e	ν_μ	ν_t	0
Quarks	u	c	t	2/3
	d	s	b	- 1/3

Fermions are the half - integer spin particles and described by the Fermi - Dirac statistics. The quarks and leptons are building block of matter and antimatter [1 - 3]. In the SM, the base exchange is the gluon which mediates the forces between quarks. Bosons are identical particles having zero of integer spin. Behaviors of bosons are described by the Bose - Einstein statistics. The SM [2 - 4] only consists of five elementary bosons and twelve of leptons and quarks. Besides that there are gluons and Higgs boson (Fig. 2).

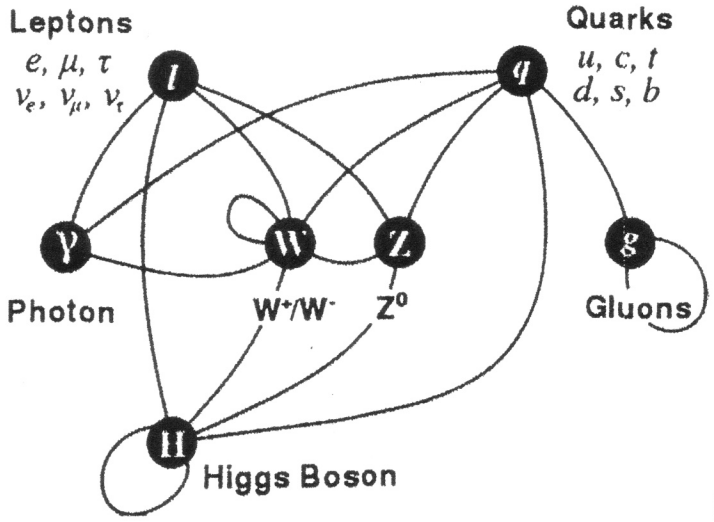

Fig. 2. Summary of interactions between particles described by the Standard Model.

According to contemporary physics the strong force does not act on lepton (electrons, positrons, muons and neutrinos), but only on protons and neutrons (more generally, on baryons and mesons - this is the reason for the collective name hadrons) (see, however below). It should be add that the forces between the quarks must be long range, because the gluons (as photons) have zero mass. This does not imply that the forces between hadrons are also long - range, because hadrons have zero color charges overall. The forces between the colorless hadrons are the residues of the for as between their quark constituents, and cancel when the hadrons are far apart [2 - 4]. In 1935, Yukawa [7] pointed out that the nuclear force could be generated by the exchange of a hypothetical spinless particle, provided its mass intermediate between the masses of proton and electron - a meson. Yukawa predicted the pion [1 - 4].The macroscopic manifestations of the strong interaction are restricted up to now to radioactivity and the release of nuclear energy. Yutaka's potential has the form[4, 5]

$$V = g\frac{e^{-kr}}{r^n}, \qquad (3)$$

for some n. Here the strength of the force is measured by the constant k (see, also [5]). The most important feature Yukawa's forces is that they have a small range (~ 10^{-15} m). The central dogma of atomic physics after Yukawa's paper that proton -

electron attraction could be explained in terms of classical electrostatic theory, while the strong force effects were essentially new and inexplicable. So, far the best theoretical guess is the Yukawa potential, but it is a static potential not dependent on velocities of the nucleons. A static force is not a complete one because it can not explain the propagation of the nuclear interaction. Moreover, as was indicated above, a phenomenological Yukawa potential can not be directly verified experimentally. We should note that nowadays in text books and elsewhere the separation of electromagnetic and strong interaction tacitly assumed. It is very strange up to present time we do not even know the strong force very well. And what is more we have some contradiction taking into account that the forces between quarks must be long - range, because the gluons have zero mass. But as was mentioned above the force between colorless hadrons is short - range, when the distance between hadrons is more than nuclear size [1, 7].

Table 2. The four fundamental forces.

Interaction	FQ	Mass	Range (m)	RS	Spin	TC-S (m^2)	TTS(s)
Str	Gluon	0	10^{-15}	1	1	10^{-30}	10^{-23}
We	W , Z	81, 93 GeV/c2	10^{-18}	10^{-5}	1, 1	10^{-44}	10^{-8}
Elec	Photon	0	∞	1/137	1	10^{-33}	10^{-20}
Gra	Graviton	0	∞	10^{-38}	2	-	-

Here - FQ field quant, RS relative strength, TC - S Typical cross - section, TTS - Typical time scale.

The Table 2 (see also [2, 4]) given for the strength and range of the forces come from a comparison of the effects they produce on two protons. In some respect these resemble an ordinary Newtonian force between the protons, varying with the distance between them as if the force was derived from a potential function (1): for some n. This is an inverse - power force which is diminished by an exponential factor at distances larger than a certain distance R, the range of the force. The strength of the force is measured by the constant k. The unit of strength is $hc/2\pi$ where h is Planck's

constant and c the speed of light. Thus nuclear physics was essentially the paradigmatic example of understanding particle physics. The modern quantummechanical view of the three fundamental forces (all except gravity) is that particles of matter (fermions neutrons, protons, electrons) do not directly interact with each other, but rather carry a charge, and exchange virtual particles (gauge bosons photons, gluons, gravitons) which are the interaction carriers or force mediators. As can be seen from Table 2, photons are the mediators of the interaction of electric charges (protons, electrons, positrons); and gluons are the mediators of the interaction of color charges (quarks). In our days, the accepted view is that all matter is made of quarks and leptons . As can be seen, of the three pairs of quarks and leptons, one pair of each - the quark u and d and the leptons e^- and ν_e (electrons neutrino) - are necessary to make up the every day world, and a world which contained only these would seem to be quite possible.

As we can see above the method of the scattering particles allows to determine only length of scattering as well as the size and depth (highest) of the neutron's potential. In the present paper we attempt to measure the energy of the neutron - electron interaction via spectroscopic study of the optical characteristics of solids with isotope effect at low temperature. Therefore, it is purpose of our paper to advance a description of the manifestation of strong nuclear interaction in solids, using partly published and new non - accelerator experimental results. Our spectroscopic measurement of the low temperature optical characteristics of LiH_xD_{1-x} crystals is permitted to quantitative study of the dependence of strong coupling constant, α_s, on the proton - neutron distance in the deuteron nuclei. Carbon, being the second element after silicon on Earth, has unusually wide range of allotropic compounds with completely different physical properties [8]. The use of our object allows the investigation of not only the isotope effects in lattice dynamics (vibrational, elastic and thermal properties), but also the influence of such effects on the electronic excitations (for example, the renormalization of the band - to - band transition energy E_g). We emphasize that the study of the isotope effect remains at the forefront not only in materials science, but also nuclear and high energy physics. In connection with of our analysis, we must emphasize that outstanding works on strong interaction in hadrons mechanics deserve separate and fundamental study [9]. A detailed comparison with the theory of hadron mechanics [9] and interpretation will be given in the forthcoming paper (see also [10] and referencies therein).

II.Experimental.

Below we briefly describe the results of the low - temperature optical spectroscopy of isotope - mixed solids. The apparatus used in our experiments has been described in several previous publication [10 - 12]. For clarity, we should mentioned here that immersion home - made helium cryostat and two identical double - prism monochromators were used. one monochromator was used for the excitation and the other, which was placed at right - angle to the first for analyzing the luminescence and scattering of light. In our experiments we investigated two kinds of crystals (LiH and LiD) which are differ by a term of one neutron. Lithium hydride and lithium deuteride are ionic insulating crystals with simple electronic structure, four electrons per unit cell, both fairly well – described structurally (neutron diffraction) and dynamically (second – order Raman spectroscopy) and through ab initio electronic structure simulation. Among other arguments, LiH and LiD are very interesting systems due to their extremely simple electronic and energy structure and to the large isotopic effects when the hydrogen ions are replaced by the deuterium ones. On the other hand, the light mass of the ions, specially H and D, makes that these solids have to be considered like quantum crystals, and consequently, described theoretically by quantum theory. In a solid one deals with a large number of interacting particles, and consequently the problem of calculating the electronic wave functions and energy levels is extremely complicated. It is necessary to introduce a number of simplifying assumptions. In the first place we shall assume that nuclei in the crystalline solid are at rest. In an actual crystal this is of course never the case, but the influence of nuclear motion on the behavior of electrons may be treated as a perturbation for the case in which they are assumed to be at rest. Even with above assumption, however, we are still with a many – electron problem which can be solved only be approximative methods. In the case of solids, the most important approximative method which has been applied extensively is the so – called one – electron approximation. In this approximation the total wave function for the system is given by a combination of wave functions, each of which involves the coordinates of only one electron. In other words, the field seen by a given electron is assumed to be that of the fixed nuclei plus some average field produced by the charge distribution of all other electrons [13].

The difference between a good conductor and a good insulator is striking. The electrical resistivity of a pure metal may be as low as 10^{-10} ohm-cm at a temperature of 1 K, apart from the possibility of superconductivity. The resistivity of good

insulator may as high as 10^{22} ohm-cm. The understand the difference between insulators and conductors, we shall use the band – gap picture (Fig. 3 below). Since atom are located in space strictly periodically in the crystal, the full potential $V(\vec{r}) = \tilde{U}_i(\vec{r}\ ) + U(\vec{r})$ must have a three - dimensional periodicity (here $U_i(\vec{r}$ and $U(\vec{r})$ are potential energy if i - electron and all others). Although the exact species $V(\vec{r})$ is unknown, it is important to know that this potential is a periodic function whose period coincides with the period of the crystal lattice of the object under study. This periodicity leads to the formation of a band energy structure (Fig. 3). An electron from the valence band (see Fig. 3) is excited into the conduction band. The possibility of band gap is the most important property of solids.

The single crystals of LiH and LiD were grown from the melt by the modified method of Bridgeman - Stockbarger (see [14, 15] and references quoted therein). The crystals were synthesized from ^{7}Li metal and hydrogen of 99.7% purity and deuterium of 99.5% purity. Virgin crystals had a slightly blue - grew color, which can be attributed to nonstoichiometric excess of lithium present during the grown cycle. On annealing for several days (up to 20) at 500^0C under ~ 3 atm of hydrogen or deuterium, this color could be almost completely eliminated. Because of the high reactivity and high hygroscope of investigated crystals an efficient protection against the atmosphere was necessing. Taking into account this circumstance, we have developed special equipment which is allowed to prepare samples with a clean surface cleaving their in the bath of helium cryostat with normal or superfluid liquid helium [10]. The samples with such surface allow to perform measurements during 15 hours. An improved of LiH (LiD) as well as mixed crystals were used in the present study. In spite of the identical structure of all free - exciton luminescence spectra, it is necessary to note a rather big variation of the luminescence intensity of the crystals from the different batches observed in experiment.

We should remind very briefly about the electronic excitations in solids. According to modern concept, the excitons can be considered [13] as the excited of the N - particles system: An electron from the valence band (see Fig. 3) is excited into the conduction band.

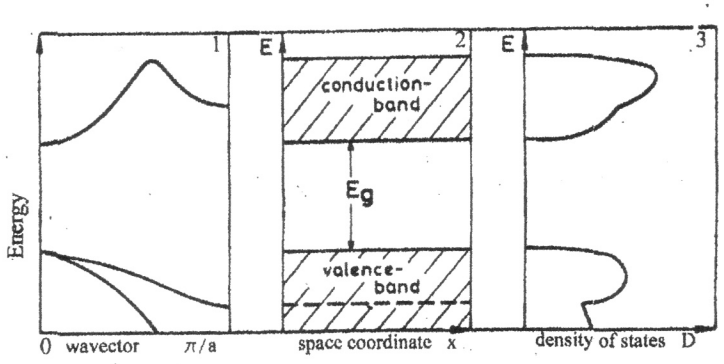

Fig. 3. Various possibilities to present the band - structure of homogeneous, undoped insulator (semiconductor). 1 - the dispersion relation, i.e. the energy E as a function of the wave vector $\vec{k}$, 2 - the energy regions of allowed and forbidden states as function of a space coordinate x and , 3 - the density of states (all curves are schematic ones).

The attractive Coulomb potential between the missing electron in the valence band, which can be regarded as a positively charged hole, and the electron in the conduction band gives a hydrogen - like spectrum with an infinitive number of bound state and ionization continuum (Fig. 4).

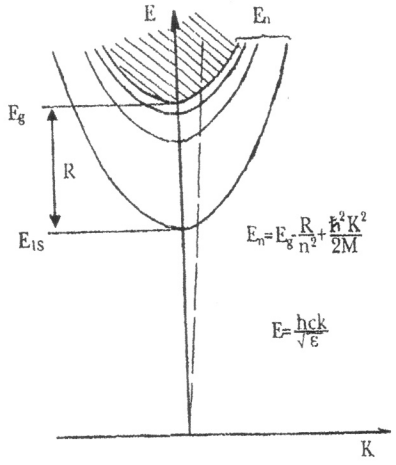

Fig. 4. Discrete and continuos (hatched area) Wannier - Mott exciton energy spectrum taking into account its kinetic energy. The broken line connects to the dispersion of light in the medium. R - is the exciton binding energy, n = 1, 2, 3, ...

In our short review we call the bound states of electron - hole (e - h) pairs exciton states (exc), while we refer to ionized e - h pairs as free carriers. however, the expression free carriers does not imply that the effect of the strong Coulomb forces between electronic excitation could be neglected. Thus, an exc - state can be built by appropriate superposition of e - h pairs, which in a simple two - band model for cubic crystal symmetry is given (more details see [10]). In our experiments we have investigated the low - temperature optical spectra (reflection, photoluminescence and scattering of light) of LiH_xD_{1-x} crystals ($0 \leq x \leq 1$) which are differ by term of one neutron from each other.

Spectra were excited by various lines of a 400 W deuterium lamp and a 120 W mercury arc lamp (see Fig. 5). The excitation light was felt on the entrance slit of the first monochromator and after leaving it passed through quartz windows of the immersion helium cryostat and irradiated of the crystals. The luminescence and scattering light from the samples was dispersed in another double prism (grating) monochromator and photoelectrically detected. A photoelectric registration of the optical signal was realized by a cooled photopmultiplier for ultraviolet (UV) range of the spectrum and the subsequent high - sensitivity photon - counting system with a

storage facilities (computer). The signal - to - noise ratio was approximately $n \cdot 10^2$ where $n = 2 \div 5$ for different batches of crystals. The light scattering experiments were performed in the usual backscattering geomentry, at temperatures of 2 to 300 K. To allow for the $\approx \omega^4$ law, a freshly cleaved of LiF crystal was used, whose dispersion of the refractive index in the spectral region 4 to 6 eV is small. The experiments were carried out in the same way for two (LiH and LiD) compounds, which differ by a term of one neutron.

An improved of LiH (LiD) crystals were used in the present study. In spite of the identical structure of all free - exciton luminescence spectra, it is necessary to note a rather big variation of the luminescence intensity of the crystals from the different batches observed in experiment.

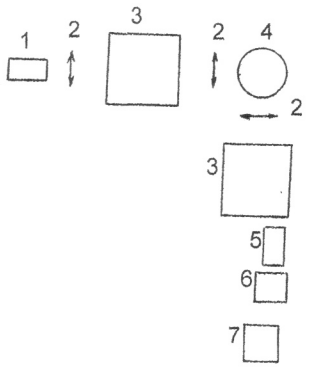

Fig. 5. Scheme of experimental setup: 1 - lamp, 2 - lens, 3 - monochromator, 4 - He cryostat, 5 - photomultiplier, 6 - photon counter, 7 - personal computer.

III. Results.

The usual way to determine the optical properties of a solid is to shine monochromatic light onto an appropriate sample and then to measure the reflectance or transmittance of the sample as a function of photon energy. In the spectral region of greatest interest is generally quite high, so that often a negligible small fraction of the incident light is transmitted. It is the main reason, that the most experiments are

measurements of the reflectivity. The mirror reflection spectra of mixed and pure LiH and LiD crystals, cleaved in superfluid helium are presented on Fig. 6. All spectra have been measured with the same apparatus under the same conditions. As can clearly seen in Fig. 6 all spectra exhibit a similar long – wave structure. As the deuterium concentration increases, the long – wave maximum (n = 1S excitons [10, 13]) broadens and shifts towards the shorter wavelengths. The energy values of exciton maxima for pure and mixed crystals at 2 K are presented in Table 2.

Table 3. Values of the energy of maxima (E_1 and E_2) (in meV) in exciton reflection spectra of pure and mixed crystals at 2 K, and energies of exciton binding energy E_b, band - to - band transitions E_g.

	LiH	$LiH_{0.82}D_{0.18}$	$LiH_{0.40}D_{0.60}$	LiD	Li^6H (78 K)
E_1	4950	4967	5003	5043	4939
E_2	4982	5001	5039	5082	4970
E_b	42	45	48	52	41
E_g	4992	5012	5051	5095	4980

As demonstrated early (see, e.g. book [15) most low - energy electron excitation in LiH crystals are the large - radius excitons [13].

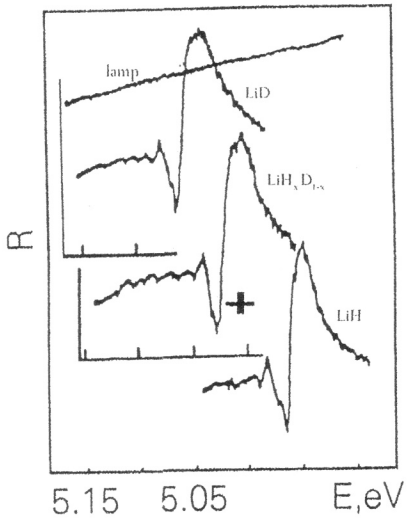

Fig. 6. Mirror reflection spectra in indicated crystals at 2 K cleaved in superfluid helium. Light source without crystals, curve lamp.

Going back to Fig. 6, it is hard to miss the growth of Δ_{12}, which in hydrogen - like model [13] causes an increase in exciton Rydberg (E_b) with the replacement of isotopes (for details see [15]). The single - mode nature of exciton reflection spectra of mixed crystals LiH_xD_{1-x} agrees qualitatively with the results obtained with the virtual crystal model [16]. All of these results are documented in Table 2, where the variation of E_g, E_b are shown at the isotope effect. We should highlight here that the most prominent isotope effect is observed in LiH crystals, where the dependence of $E_g = F(C_D)$ is also observed and investigated (see below Fig. 9).

Photoluminescence is the optical radiation emitted by a physical system (in excess of the thermal equilibrium blackbody radiation) resulting from excitation to a nonequilibrium state by irradiation with light. Photoluminescence is also rapidly evolving into major basic research tool comparable to absorption (reflection) measurements in importance. Two reason for this stand out as significant. First is the sensitivity of the luminescence technique. It often happens that features which are just discernible in absorption will completely dominate the luminescence spectra. The converse is also sometimes true, making luminescence and absorption (reflection) complementary techniques. Second is the simplicity of data collection. In last half-century the luminescence method has become one of the most common techniques for studying excitons in dielectrics and semiconductors. While the structure of spectra of fundamental reflection (absorption) depends on the internal degrees of freedom of Wannier – Mott exciton, the structure and shape of the luminescence spectrum are determined primarily by its external degrees of freedom. The latter are associated with the translation motion of large – radius exciton as a whole, with the translation mass $M = m_e + m_h$, where m_e and m_h – effective masses of electron and hole, respectively.

Free exciton luminescence is observed when LiH (LiD) crystals are excited in the midst of the fundamental absorption. The spectrum of free exciton photoluminescence of LiH crystals cleaved in superfluid helium consists of a narrow (in the best crystals, its half - width is $\Delta E \leq 10$ meV) phononless emission line and its broader phonon repetitions, which arise due to radiated annihilation of excitons with the production of one to five longitudinal optical (LO) phonons (see Fig. 7).

The phononless emission line coincides in an almost resonant way with the reflection line of the exciton ground state which is indication of the direct electron transition $X_1 - X_4$ of the first Brillouin zone [17].The lines of phonon replicas form

an equidistant series biased toward lower energies from the resonance emission line of excitons. The energy difference between these lines in LiH crystals is about 140 meV, which is very close to the calculated energy of the LO phonon in the middle of the Brillouin zone [18] and which was measured early (see, e.g. [15] and references quoted therein). The isotopic shift of the zero - phonon emission line of LiH crystals equals 103 meV. As we can see from Fig. 7 the photoluminescence spectrum of LiD crystals is largely similar to the spectrum of intrinsic luminescence of LiH crystals. There are, however, some distinctions one is related. Firstly the zero - phonon emission line of free excitons in LiD crystals shifts to the short - wavelength side on 103 meV. These results directly show the violation of the strong conclusion (see, e.g. [1, 2, 4]) that the strong force does not act on leptons. The second difference concludes in less value of the LO phonon energy, which is equal to 104 meV. The simplest approximation, in which crystals of mixed isotopic composition are treated as crystals of identical atoms having the average isotopic mass, is referred to as virtual crystal approximation (VCA) [15].

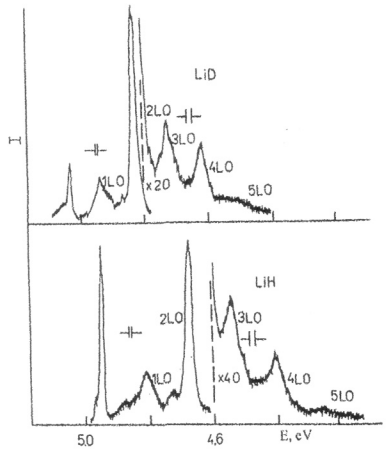

Fig. 7. Photoluminescence spectra of free excitons at 2 K in LiH and LiD crystals cleaved in superfluid helium.

When light is excited by photons in a region of fundamental absorption in mixed LiH_xD_{1-x} crystals at low temperature, line luminescence is observed (Fig. 8), like in the pure LiH and LiD crystals. As before [15], the luminescence spectrum of crystals

cleaved in superfluid liquid helium consists of the relatively zero - phonon line and its wide LO replicas. For the sake of convenience, and without scarfing generality, Fig. 8 shows the lines of two replicas. Usually up to five LO repetitions are observed in the luminescence spectrum as described in detail in [18, 14]. In Fig. 8 we see immediately that the structure of all three spectra is the same. The difference is in the distance between the observed lines, as well as in the energy at which the luminescence spectrum begins, and in the half - width of the lines (see, also Table 3).

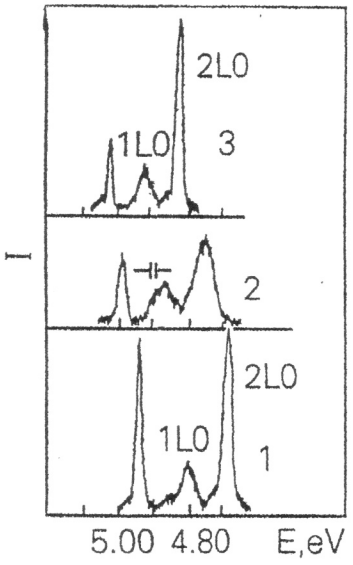

Fig. 8. Photoluminiscence spectra of free excitons in LiH (1), LiH_xD_{1-x} (2) and LiD (3) crystals cleaved in superfluid helium at 2 K. Spectrometer resolution is shown.

At the excitation below the intrinsic absorption edge ($E_{n=1s}$ = 5.043 eV for LiD [19]) we have succeeded in observing the multiphonon resonance Raman scattering (RRS) with the creation of up four phonons (Fig. 9). Indeed, the energy difference between peaks in the RRS spectrum is equal the energy of the LO phonons in the center of the Brillouin zone [18, 14].

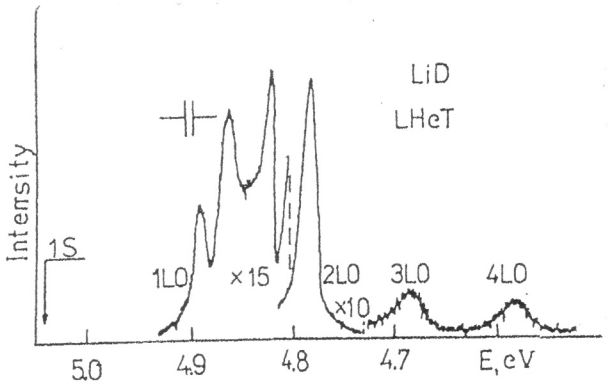

Fig. 9. Resonant Raman scattering of a LiD crystals at the excitation E = 4.992 eV at 4.2 K.

To pay attention the large half - width of observable lines in the RRS spectrum. As was shown in the paper [20] their half - width are always larger than of the excitation line. The proximity of the exciting light frequency to the energy of exciton transitions leads to an essential modification of the selection rules for light scattering. The presence of the second - order TO (Γ) ($\hbar\omega_{TO(\Gamma)}$ = 76 meV for LiH) in the RRS spectrum may be explained by a relatively strong scattering deformation mechanism in these crystals, where, however the main mechanism, as was seen from both figures, is Frőchlich mechanism of intraband scattering. The longwavelength displacement of the excitation line frequency relatively exciton resonance a monotonic decrease the intensity of RRS spectrum as whole more than 60 - fold in both LiH and LiD crystals [15].

The X - Ray diffraction investigaions show [21] that LiH_xD_{1-x} mixed crystals form a continuos row a variable lattice constant (and exciton radius, respectively) that obeys Vegard's law [16].

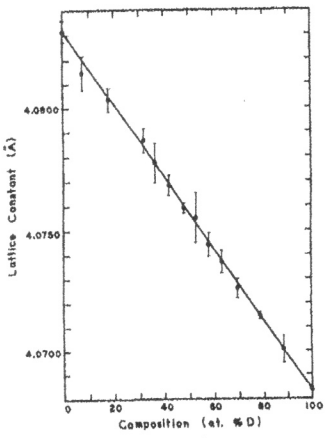

Fig. 10. Lattice constant in the ^{7}Li(H, D) crystals plotted against the isotopic concentrtion (after [21]).

Taking into account linear dependence on the lattice constant (Fig. 10) we have build the dependent of the band gap energy on the distance between nucleons in deuterium nuclei. Fig. 11 shows the concentration dependence of the energy of interband transition E_g (force of strong interaction between proton and neutron) (see Fig. 2). As can be seen from Fig. 11, VCA method (the straight dashed line) cannot describe observed experimental results. This dependence has a nonlinear character. Here r_H and r_D are radius of hydrogen and deuterium nuclei according to CODATA data.

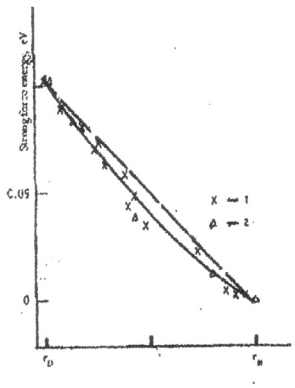

Fig. 11. The long – range part of the force of strong nuclear interaction dependence on the distance between nucleons in deuterium nucleus. The straight dashed line is the linear dependence of the force dependence F_s in the virtual model. The solid line corresponds to calculation using the polynom of second degree $F_s = f(r_d)$. Points derived from the reflection spectra indicated by crosses, and those from luminescence spectra by triangles.

Comparison the all experimental results on the luminescence (reflection) and light scattering in the crystals which differ by a term of one neutron only is allowed to the next conclusions;

1. At the adding one neutron (using LiD crystals instead LiH ones) is involved the increase exciton energy on 103 meV.
2. At the addition one neutron the energy of LO phonons is decreased on the 36 meV, that is direct seen from luminescence and scattering spectra.
3. In the isotope effect, the energy of acoustic phonons does not depend on the replacement of H by D [20] , which is proved by identical structure of the light scattering spectra [15, 22]. Along with this, a small change in the energy of optical (LO) phonons (36 meV) observed in the luminescence and light scattering spectra indicates a non - electron - phonon renormalization mechanism of the energy of zero - phonon line of free excitons in LiD crystals.

Both characteristics are macroscopic. As will be shown below these experimental results are very useful for nuclear and physics of high energy physics.

IV. Discussion.

Traditionally nuclear - electron interaction (in our case neutron - electron interaction) taking into account the solving Schrödinger equation using Born - Oppenheimer (adiabatic) approximation [23]. Below we consider the essence of the Born - Oppenheimer approximation of the nuclear - electron interaction on the molecule example. The Schrödinger equation for the molecule

$$\hat{H}\Psi(\vec{r}, \vec{R}) = E\Psi(\vec{r}, \vec{R}) \qquad (4)$$

here $\Psi(\vec{r}, \vec{R})$ is an eigenfunction and E the corresponding eigenvalue, $\hat{H}$ the Hamiltonian operator of molecule and $\vec{r}$ is electron and $\vec{R}$ is nuclear distance. The simplest approximate method for solving the Schrödinger equation (4) uses, as indicated above, the so - called Born - Oppenheime approximation [23]. This approximation is used that the nuclei are much heavier than an electron and, consequently, move very slowly in comparison with the electronic motion.

If the nucleus to be fixed in some configuration for this particular $\vec{R}$ (distance between nuclei) we get the next differential equation

$$-\frac{\hbar^2}{2m}\sum_i \Delta_i^2\Psi(\vec{r}, \vec{R}) - \frac{\hbar^2}{2}\sum_\alpha \frac{\Delta_\alpha}{M_\alpha}\Psi(\vec{r}, \vec{R}) + V(\vec{r}, \vec{R})\Psi(\vec{r}, \vec{R}) = E\Psi(\vec{r}, \vec{R}), \quad (5)$$

where Δ is Laplasian [24], m and M electron and nucleus mass, index i for electrons and α is index for nuclei.

Further we put

$$\Psi(\vec{r}, \vec{R}) = \chi(\vec{r}, \vec{R})\varphi(\vec{R}) \qquad (6)$$

here $\varphi(\vec{R})$ is the nuclear wavefunction, which depends on nuclear distance $\vec{R}$ and on electronic state.

After substitution (6) in (5) we have

$$-\frac{\hbar^2}{2m}\varphi(\vec{R})\sum_i \Delta_i\chi(\vec{r}, \vec{R}) - \frac{\hbar^2}{2}\sum_\alpha \frac{\Delta_\alpha}{M_\alpha}\chi(\vec{r}, \vec{R})\varphi(\vec{R}) + V(\vec{r}, \vec{R})\chi(\vec{r}, \vec{R})\varphi(\vec{R}) = E\,\chi(\vec{r}, \vec{R})\varphi(\vec{R}). \qquad (7)$$

Further we neglect the next members in (7)

$$\hat{L}\Psi(\vec{r}, \vec{R}) = -\frac{\hbar^2}{2}\sum_\alpha \frac{1}{M_\alpha}[\varphi(\vec{R})\Delta_\alpha\chi(\vec{r}, \vec{R}) + 2\nabla_\alpha\varphi(\vec{R})\nabla_\alpha\chi(\vec{r}, \vec{R})]. \qquad (8)$$

Operator $\hat{L}$ is call the non - adiabatic operator, which describe the nuclear - electron interaction. After the last operation the equation (8) splits on two equations:

$$-\frac{\hbar^2}{2m}\sum_i \Delta_i\chi(\vec{r}, \vec{R}) + V(\vec{r}, \vec{R})\chi(\vec{r}, \vec{R}) = E_l(\vec{R})\chi(\vec{r}, \vec{R}); \qquad (9)$$

and

$$-\frac{\hbar^2}{2}\sum_\alpha \frac{\Delta_\alpha}{M_\alpha}\varphi(\vec{R}) + E_l(\vec{R})\varphi(\vec{R}) = W\varphi(\vec{R}). \qquad (10)$$

Where $E_l(\vec{R})$ is electronic energy and W is the nuclear energy. Every equation have the view of the Schrödinger equation. The first equation (9) describes the electron stationary state in adiabatic approximation. Equation (10) is an equation for a wavefunction of the nuclei alone. Note, please that Equation (9) contains the nuclear charges through the Coulomb potential, but is doesn't include any reference to nuclear mass. Thus $E_l(\vec{R})$, the eigenvalue (energy) of the electronic Schrödinger equation (9) is the same for all isotopes, and consequently, is isotopically independent. The independent $E_l(\vec{R})$ on isotopic substitution is the essence of the Born - Oppenheimer approximation. However, we must repeat, that the Born - Oppenheimer approximation

[23] is the standard anzatz to the description of the interaction between electrons and nuclei in solids (see, e.g. [25]). Moreover, comparison the non - accelerator experimental results on the luminescence (reflection) and light scattering [15] in the crystals which differ by a term of one neutron only is allowed to the next conclusions;

1. At the adding one neutron (using LiD crystals instead LiH ones) is involved the increase exciton energy on 103 meV.

2. At the addition one neutron the energy of LO phonons is decreased on the 36 meV that is direct seen from luminescence and scattering spectra [20].

3. In the isotope effect, the energy of acoustic phonons does not depend on the replacement of H by D [15, 20], which is proved by the identical structure of the light scattering spectra [15, 19, 22]. Along with this, a small change in the energy of optical (LO) phonons (36 meV) observed in the luminescence and light scattering spectra indicates a non - electron - phonon renormalization mechanism of the energy of zero - phonon emission line of free excitons in LiD crystals. The same results have been obtained for diamond.

The X - ray diffraction investigations show that the LiH_xD_{1-x} mixed crystals [21] form a continuos row of the solid solution and testify themselves like a virtual crystal with a variable lattice constant (and exciton radius, respectively) that obeys Vegard's law (see Fig. 10).

The measurements of the low temperature of reflection [15, 19, 22] and luminescence spectra of the whole series of mixed crystals is permitted to obtain the dependence of the interband transition (the long - range force dependence of strong nuclear interaction on the distance between nucleons in deuterium nucleus) energy on the deuterium concentration (see below Fig. 11). Taking into account that the concentration of the isotopes is vary directly the lattice constant (see Fig. 36) we are plotting the dependence of the power of the force strong interaction on the distance between nucleons depicted on Fig. 11. This dependence has a nonlinear character. As can be seen from Fig. 11, VCA method (the straight dashed line) cannot describe observed experimental results.

The independent of the potential energy (the eigenvalue of the Schrödinger equation) is the essence adiabatic approximation. However, we must repeat, that the Born - Oppenheimer approximation [20] is the standard anzatz to the description of the interaction between electrons and nuclei in solids [25]. Now we should take into account a small contribution to isotopic shift through reduced electron mass $\mu = ((m_e M_{Nucl})/(m_e + M_{Nucl}))$ so far as M_{Nucl} is different for the hydrogen and deuterium nucleus. In this case the contribution equals $\Delta E \simeq 6$ meV. Contribution to isotope shift of the zero - phonon line in luminescence spectra of LiD crystals as well as Lamb shift

and specific Coulomb potential approximately equal 1, and 1 meV, respectively. This values is less then isotope shift in our experiments on the two order and more. These all last results force us to search for new models and mechanisms of nuclear (neutron) - electron interaction including the results of subatomic physics, e.g. hadron - lepton interaction.

Out of four known interactions, three are described by SM - the electromagnetic, weak and strong ones. The first two of them have a common electroweak gauge interaction behind them. The symmetry of this interaction $SU(2)_L$ X $U(1)_Y$ manifests itself at energies higher than ~ 200 GeV. At lower energies, this symmetry is broken down to $U(1)_{EM} \neq U(1)_Y$ (the electroweak symmetry breaking): in SM this breaking is related to the vacuum expectation value of a scalar field [26]. The strong interaction in SM is described by the QCD, a theory with the gauge group $SU(3)_C$. The effective coupling constant of this theory grows when the energy decreased [1]. As a result, particles which feel this interaction cannot exist as free states and appear only in the form of bound states called hadrons (see, also [26]). Most of modern methods of quantum field theory work at small values of coupling constant,α_s, [27 - 31], that is, for QCD, at high energies. Quarks and leptons, the so - called SM matter fields, are described by fermionic fields. Quarks take part in strong interactions and compose observable bound state hadrons. Both quarks and leptons participate in the electroweak interaction. The matter fields constitute three generation: particles from different generation interact identically but have different masses (see, e.g. [4]). For the case of neutrino, Yukawa [7] interactions are forbidden as well, so neutrinos are strictly massless in SM (see, however [32]). The gauge bosons, which are carriers of interactions, are massless for unbroken gauge groups $U(1)_{EM}$ (electromagnetism - photons) and $SU(3)_C$ (QCD - gluons), masses of $W^{\pm}$ and Z^0 bosons are determined by the mechanism of electroweak symmetry breaking. It should noted that the forces between the quarks must be long - range, because the gluons have zero mass. This does not imply that forces between hadrons are also long range, because hadrons have zero color charges overall. The forces between the colorless hadrons are the residues of the forces between their quark constituents, and cancel when the hadrons are far apart.

Returning to our non - accelerator experimental results, we should underline that in this paper we measure the strong coupling strength in crystals which differ by term of one neutron from each other. When we add one neutron in the hydrogen nucleus, we artificial activation of the strong interaction. As far as the gravitation, electromagnetic and weak interactions are the same in both kind crystals (LiH and LiD), it only changes the strong interaction. Therefore a logical conclusion is made that the

renormalization of the energy of electromagnetic excitations (isotopic shift equals 0.103 eV) is carried out by strong nuclear interaction. The short - range character of the strong interaction of nucleons does not possess direct mechanism of the elementary excitation (electrons, excitons, phonons) energy renormalization, which was observed in our low temperature experiments. Second reason that the interpretation of our experimental results is very difficult task because they are first demonstration of the violation of the strong conclusion in nuclear and particles physics that the strong nuclear force does not act on the colorless leptons (see, e.g. [4, 1]). Moreover we have some contradictions taking into account that the forces between quarks must be long - range, because the gluons have zero mass. But as was mentioned above, the short range when forces between the colorless hadrons are the residues of the forces between their quark constituents, and cancel when the distance between hadrons is more than nuclear size [5]. We can see that the nuclear size transforms long - range interaction in the short - range strong one. It is very old question which up to present time has not any theoretical explanation.

In spite of above discussion, at present time we can distinguish the following mechanisms of the isotopic shift zero phonon line:

1. Long - range electric field of the neutron's quarks. This mechanism owing to the confinement quarks is limited by the boundary of the neutron.

2. The possible new structure of the quarks and leptons - so - called preons [1, 33 - 38].

3. The most likely mechanism of the neutron - lepton interaction is connected to the magnetic - like strong field of neutron 's quarks. Taking into account anomalous magnetic moment of the neuron in the paper [39] was obtained the value of strong coupling constant $\alpha_s = 2.4680$ (see, also[40]). Quite large value in comparison with the accelerator technique value $\alpha_s(M_Z) = 0.1198$ [28]. The large value α_s is thus justified to think that residual strong forces acting beyond nucleon could exist. A possible interpretation is to assume that in addition to the 8 gluons predicted by QCD $SU(3)_c$ group there is a ninth gluon color singlet [4]

$$g_9 = \frac{1}{\sqrt{3}} (r\bar{r} + g\bar{g} + b\bar{b}) \qquad (11)$$

This massless photon - like gluon may be strongly interacts between nucleons (neutrons) and leptons (electrons) (see, also [2, 4]. Returning to Fig. 11 we can note that our measurements permit to obtain value of strong coupling constant from $\alpha_s =$

2.4680 (pure LiD crystals) to $\alpha_s = 0$ (pure LiH crystals). Moreover, in Fig. 12 we show the dependence of α_s on neutron's number in different substances. We can see as early in the case of pure LiD crystals we have non - linear character of α_s on the neutron's number in different substances. Deviation from nonlinearity may indicate the emergence of a new force not taken int account in the SM and requiring a more fundamental, including theoretical analysis.

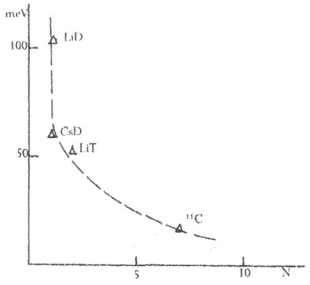

Fig. 12. The dependence of the strong force on the number of neutrons in different substances.

Thus, the tentative interpretation of describing non - accelerator experimental results does not find consisted explanation at the change of strong interaction leaving to another mystery of SM. We should remind that intrinsic contradiction of Standard Model is already well - known. Really, the Lagrangian of QCD (theory of the strong interaction) has the next form (see, e.g. [41]):

$$L = i\sum_q \overline{\Psi}^a_q(\nabla_\mu\gamma_\mu + im_q)\Psi^a_q - \tfrac{1}{4}G^n_{\mu\nu}G^n_{\mu\nu}, \quad (12)$$

where

$$\nabla_\mu = \partial_\mu - ig\frac{\lambda^n}{2}A^n_\mu,$$

$$G^n_{\mu\nu} = \partial_\mu A^n_\mu - \partial_n A^n_\mu + gf^{nml}A^n_\mu A^l_\nu. \qquad (13)$$

Ψ^a_q and A^n_μ are quark and gluon fields, a=1,2,3,...8 are color indices , λ^n and f^{nml} are Gell - Mann matrices and f symbols, m_q - are bare (current) masses, q = u, d, s, c, ... different quarks. It is common place [2, 4] that the Lagrangian (12) contains the members which describe both free motion and interaction between quarks and gluons, which is defined by the strength couple g. Spacing of which it is necessary to remark that although the Lagrangian (12) possesses rather attractive peculiarities (see, also [2, 4]), its eigenstates are the quarks and the gluons which are not observed in free states [42, 43]. The observed hadrons in the experiment don't eigenstates in QCD. It is obvious to expect that the modern theory of QCD should finally overcome these difficulties.

The next step our discussion is devoted to the neutron - electron binding energy. From our non - accelerator experimental results is followed that this value equals 0.106 eV on LiH_xD_{1-x} and 0.107 eV on the diamond (see, also [44]). In electrostatic model, it is shown [45] the neutron - electron binding energy is less than analogous proton with an electron (13,6 eV) by approximately 128 times. Hence it follows that the theoretical value of the binding energy of a neutron with an electron is 106, 7 meV. Our experimental value of a neutron - electron binding energy is in excellent agreement with theoretical value.

The remarkable properties of the graphene promise unheard of applications, especially in the semiconductor state. Especially graphene nanostructures are promising candidates for future nanoelectronics and solid - state quantum information technology. As was shown above, in the vicinity of K - points (Fig. 5 in Chapter 5 [1]), the low - energy electron/hole dispersion relation is proportional to momentum, rather than its square (see, e.g. [46, 47]). This is analogous to the energy dispersion relation of massless relativistic electrons, so the electrons/holes of graphene are described as Dirac fermions having no mass. In a simple neighbor model graphene is a semimetal with zero - overlap between valence and conduction bands. In order to make graphene a real technology, a special issue must be solved: creating an energy gap at K - points in the Brillouin zone (see, Fig. 5 in Chapter 5 [1]).

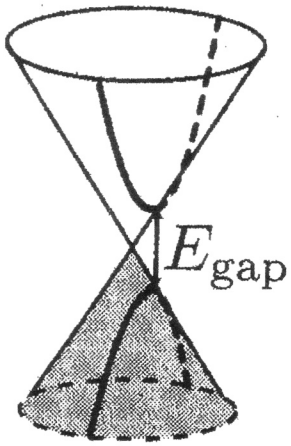

Fig. 13. The energy dispersion of semimetal (solid line) and semiconductor (dashed line).

Different attempts have been made by researches, such as patterning graphene into nanoribbon, forming graphene quantum dots, making use of multilayer graphene sheet and applying an external electric field (see, e.g [47]. It was shown that the uniaxial strain can open a band - gap in a metallic carbon nanotubes as well as carbon nanoribbon . As an example Fig. 40 shows the dependence of the energy of interband transition on the width of the graphene nanoribbons. The observed dependence is well described by the following expression $E_g = \alpha^*/ (W - W^*)$, where $\alpha^* = 0.38$ eV/nm, and $W^* = 16$ nm accounts for inactive edges [48]. This formula gives value of E_g equal to several eV, if W is reduced to a size , for example, ^{13}C, but it is impossible. The isotopic transformation of graphene, a semimetal into semiconductor deserves special attention [49, 50] This means of the cones dispersion pattern $E(\vec{k})$ at the K point of the Brillouin zone of graphene reformes into the usual parabolic dispersion of band structure pattern (see Fig. 13).

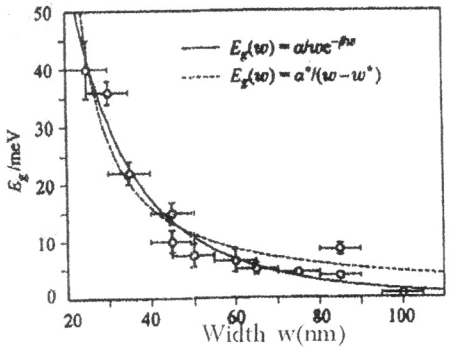

Fig. 14. The dependence of E_g as a function of width of the graphene nanoribbons (after [48]).

Taking into account Raman scattering spectra we have been obtained E_g in graphene of several hundred meV (up to 1 eV). Since value of E_g depends on the concentration of ^{13}C in graphene, this mechanism is easily realized either chemically or technologically. With the opening E_g of massless fermions (leptons = electrons) acquire mass. Estimates of different ways of opening E_g in graphene give the following equality: $E_g = 2m$ [50]. When $E_g = 1$ eV leptons acquire a mass equal 0.5 eV - the value is not large, but finite. One of the mechanisms of acquire mass in elementary particle physics is considered in the paper [51]. This paper predicts that both quarks and gluons acquire running mass distribution in QCD, which are large at infrared momenta. The current quark of perturbative QCD evolves into a constituent quark as its momentum becomes smaller. The constituent quark mass arises from a cloud of low - momentum gluons attaching then selves to the current quark. This is DCSB: an essentially nonperturbative effect that generates a quark mass from nothing; namely it occurs even in the chiral limit. DCSB namely the generation of mass from nothing is a theoretically established nonperturbative feature of QCD. The solution of a gap equation shows that gluons are cannibals: they are particle species whose members become massive by eating each other (the details see [49 - 520=]).

5. Conclusion.

The artificial activation of the strong nuclear interaction by adding one (two or more) neutrons in atomic nuclei leads it to the direct observation of the strong interaction in low - temperature optical spectra of solids. This conclusion opens new avenue in the investigation of the constant of strong nuclear interaction in the wide value range by means the condensed matter alike traditional methods. The observation of an isotopic shift (0.103 eV) of the zero-phonon line of free excitons in the luminescence spectra of LiH (without strong interaction in the hydrogen nucleus) and LiD (with strong interaction in the deuterium nucleus) crystals was the first and direct evidence of the long-range interaction of the Yukawa potential. Indeed, in both crystals, the lithium ions, the proton and the electron are the same and, therefore, the gravitational, electromagnetic and weak interactions are the same, and the addition of a neutron, according to Yukawa, a strong interaction appears, the influence of which manifests itself in the isotopic shift. These experimental results demonstrate the neutron-electron binding energy (0.106 eV) which is in excellent agreement with the theoretical Breit estimate of 0.1067 eV Experimental observation of the renormalization of the elementary excitation energy of solids by the strong nuclear interaction stimulates its count in the process of description of the elementary excitations dynamics in quantum electrodynamics. Present review continuous to develop between nuclear and condensed matter physics, and for the first time it was shown solid - state manifestation of quantum chromodynamics.

References.

1. V.G. Plekhanov, Hadron - Lepton Interaction (LAMBERT Academic Publishing, Germany, 2021)

2. D.H. Perkins, Introduction to High Energy Physics (CUP, Cambridge, 2000).

3. W.N. Cottingham, D.A. Greenwood, An Introduction to the Standard Model of Particle Physics (CUP, Cambridge, 2007).

4. G. Griffiths, Introduction to Elementary Particles (Wiley - VCH, Weinheim, 2008).

5. E.M. Henley, A. Garcia, Subatomic Physics (World Scientific Publishing Co., Singapore, 2007).

6. 6. M. Gell - Mann, Y. Neeman. The Eightfold Way (Benjamin, Reading,Mass., 1964).

7. Y. Yukawa, On the interaction of elementary particles, Proc. Phys. Math. Soc. **17** (1935) 48 - 57.

8. J.E. Field, The Properties of Natural and Synthetic Diamond (Academic Press, New York, 1982).

9. R.M. Santilli, The physics of new clean energy anf fuels according to hadronic mechanics, J. New Energy **1** (1998) 5 - 314; Scintia **151** (2024); R.M. Santilli, Hadronic Mechanics and Einstein Determenism: a New Paradigm in Nuclear Physics (Index of Sciences, London, 2025).

10. R.M. Santilli, aparent experimental confirmation of pseudoprotons and their application to new clean nuclear energies, Int. J. Appl. Math. **9** (2019) 72 - 100; A. Muktbodh, Santilli's recovering of Einstein's determinism, Prog. Phys. **20** (2024) 26 - 32; R.M. Santilli, Hadronc Mechanics and Einsrein's Determenism: A new Paradigm in Nuclear Physics (Index of Sciences, London, 2025).

11.V.G. Plekhanov, Experimental manifestation of the effect of disorder on exciton binding energy in mixed crystals, Phys. Rev. (1996) **B53** 9558 - 9560; V.G. Plekhanov, Isotope effects in lattice dynamics, Phys. - Uspekhi (Moscow) **46** (2003) 553 - 579.

12. V.G. Plekhanov, Renormalization the energy of elementary excitations in solids by the strong nuclear interaction, Universal J. Phys. and Appl. **11** (2017) 6 - 12.

13. R.S. Knox, Theory of Excitons (Academic Press, New York - London, 1963).

14. O.I. Tuytuynnik, V.I. Tuytuynnik, F.F. Gavrilov and G.I Pilipenko, Lithium hydride single crystal grow by Bridgmen - Stockbarge method using ultrosound, J. Crystal Growth **68** (1984) 741 - 749.

15. V.G. Plekhanov, Giant Isotope Effects in Solids (Stefan University Press, La Jola, CA, 2004).

16. I. Nordheim, Zur Elektrontheorie der metalle, Ann. Phys. (Leipzig) **401** (1931) 641 - 678.

17. S. Baroni, G. Pastori Parravichini, G. Pezzica, Quasiparticle band structure of lithium hydride, Phys. Rev. B**32** (1985) 4077 - 4083.

18. J.L. Verble, J.L Warren and J.L. Yarnell, Lattice dynamics of lithium hydride, ibid, **168** (1968) 980 - 989.

19. V.G. Plekhanov, Isotopic and disorder effects in large radis exciton spectroscopy, Phys. - Uspekhi **40** (1997) 553 - 568.

20. V.G. Plekhanov, V.I. Altukhov, Lihgt scattering in LiH crystas with LO phonon emission J. Raman Spectr. **16** (1985) 358 - 365.

21. W.B. Zimmerman, Lattice constant dependence on isotopic composition in the ^{7}Li(H,D) system, Phys. Rev. B**5** (1972) 4704 - 7.

22. V.G. Plekhanov, Fundamentals and applications of isotope effect in solids, **51** (2006) 287 - 426.

23. M.Born and J.R. Oppenheimer, On the quantum theory of molecules, in, Quantum Chemistry (Classic Scientific Paper) (World Sci. Publ. Co., Singapore, 2000).

24. G. Arfken, Mathematical Methods for Physicists (Academic Press, New York and London, 1968).

25. W.A. Harrison, Electronic Structure and Properties of Solids (W.F. Freeman and Co., San Fransicko, 1980); R.M. Martin, Electronic Structure - Basic Theory and Practical Methods (CUP, Cambridge, 2004).

26. F.I. Yndurain, The Theory of Quark and Gluon Interaction (Springer, Berlin, 2013).

27. G.M. Prosperi, M. Raciti, and C. Simolo, On the running coupling constant in QCD, Prog. Part. Nucl. Phys. **58** (2007) 387 - 438.

28. A. Deur, S.J. Brodsky and G.F. Toramond, The QCD running coupling, Progress in Particle and Nuclear Physics **90** (2016)1 - 74.

29. S. Bethke, World summary of α_s (2012), Eur. Phys. J. C**64** (2012) 689 - 695.

30. G. Altarelli, The QCD running coupling and its measurements, in, Proc. Corfu Summer Institute and Workshops on Elementary Particle Physics and Gravity, ArXiv: hep - ph/1303.6065 (2013).

31. G. Altarelli, Collider Physics within the Standard Model: a Primer, ArXiv: hep - ph/ 1303. 2842.

32. J. Jaeckel, A. Ringwad, The low - energy frontier of particle physics, Annu. Rev. Nucl. Part. Sci. **60** (2010) 405 - 450.

33. O.W. Greenberg, A new level of structure, Phys. Today, **38** (1985) 22 - 30.

34. B. Robson, The Generation model of particle physics, in, Particle Physics, E. Kennedy ed. (In Tech. Open Access Publisher, Rijeka, Croatia, 2012).

35. M. Aghirescu, The Cold Genesis of Matter and Fields (Science Publishing Group, New York, 2015).

36. C.S. Kalman and I. D'Souza, Preons: Models of Leptons, Quarks and Gauge Bosons as Composite Particles (World Scientific, Singapore, 1992).

37. C.S. Kalman, Why quarks cannot be fundamental particles, Nuclear Phys. B: Proceedings Supplements **142** (2005) 235 - 237.

38. O. Consa, The Helicon: A new preon model, Prog. Phys. **14** (2019) 215 - 219.

39. V.G. Plekhanov, J.G. Buitrago, Evidence of residual strong interaction in nuclear atomic level via isotopic shift in LiH - LiD crystals, Prog. Phys. **15** (2019) 68 - 71.

40. V.G. Plekhanov, Measurements of the wide value range of strong interaction coupling constant, SSRG - IJAP **6** (2019) 32 - 37.

41. I.M. Dremin, A.B. Kaidalov, Quantum chromodynamics and the phenomenology of strong interaction, Phys - Uspekhi **49** (2006) 263 - 273.

42. D. Vretenar and W. Weise, Exploring the nucleus in the context of low - energy QCD, Lecture Notes Phys. **641** (2004) 65 - 117.

43. V.G. Plekhanov, Direct observation of the strong nuclear interaction in the optical spectra of solids, Proceed. 3rd Conf. High Energy Phys. Rome, Italy, 2017, p.46.

44. V.G. Plekhanov, Phenomenology of the origin of isotope effect, PSIJ **18** (2018) 1 - 11.

45. G. Breit, Theory of isotope shift, Rev. Mod. Phys. **30** (1958) 507 - 517.

46. A.H. Castro Neto, F. Guinea, M.N. Peres et al., The electronic properties of graphene, Rev. Mod. Phys. **81** 109 - 162.

47. A.C. Ferrari, F. Fal'ko, Jari Kinaret et al., Science and technology road map for graphene, related two - dimensional crystals, and hybrid systems, Nanoscale **7** (2015) 4598 - 4810.

48. Ch. Stampfer, S. Fringe, J. Guttinger, Transport in graphene nanostructures, Front. Phys. **6** (2011) 271 - 293.

49. V.G. Plekhanov, Chapter 1 in, Understanding Quarks, Nova Science Publishers, Inc., New York, 2021, p.p. 1 - 92.

50. Ken - ichi Sasaki, Massive Dirac Fermions Signal in Raman Spectrum of Graphene, Phys. Rev. B**97** (2018)115413 - 6.

51. C.D. Roberts, Hadron physics and QCD: Just the basic facts, ArXiv: nucl - th/ 1501.06581.

52. C.D. Roberts, Empirical consequence of emergent mass, Symmetry **12** (2020) 1468 - 1506.